RSC Advances

PAPER

View Article Online
View Journal | View Issue

Cite this: *RSC Adv.*, 2025, **15**, 26632

In situ fabrication of ZIF-8 decorated tezontle for enzyme immobilization towards biodiesel production†

Yetzin Rodríguez-Mejía,*[ab] Naveen Kumar Reddy Bogireddy,*[c] Fernando Romero-Romero,*[ade] M. V. Basavanag-Unnamatla,[ae] Vivechana Agarwal[f] and Victor Varela-Guerrero*[ade]

Efficient and cost-effective materials for enzyme immobilization have been sought to enhance the stability and recyclability of enzymes. We have developed highly efficient, stable, resistant, and reproducible biocatalysts in this work. The fabricated catalysts (ZIF-8/tezontle/lipase) are economical, stable, and obtained at room temperature. The prepared materials were confirmed through diffraction planes and crystals of ZIF-8 (hexagonal shape) on the surface with a size of *ca.* 0.715 to 1.42 μm. The characteristic elements of ZIF-8, such as N and Zn, and functional groups in the prepared composites were also analyzed. The thermal stability profiles were conducted to determine the total composition loss of the prepared material compared to pristine ZIF-8. As for the feedstock and DB, it is observed that they have an acidity index of 0.67 mg KOH per g for oil and 0.2 mg KOH per g for DB, complying with the parameters established by ASTM, while the moisture increases for the DB (0.075%) because the BD is hygroscopic. In addition, it exhibited a recyclability efficiency of 91% for the composite material compared to pristine tezontle and ZIF-8 catalysts due to its comparable porosity, surface area, and surface functional groups that allow enzyme–support binding, thereby enabling lipase recyclability. Post-biodiesel analysis confirmed the reduction in chain length during the transesterification process.

Received 17th April 2025
Accepted 17th July 2025

DOI: 10.1039/d5ra02711j

rsc.li/rsc-advances

1. Introduction

Tezontle is an igneous rock formed by solidifying molten materials from magma. It mainly comprises anorthite, magnetite, or hematite.[1,2] Tezontle is commonly used as a plant substrate[3] and a construction material due to its density and cost-effectiveness.[4,5] Currently, tezontle is used for drug removal, such as carbamazepine,[6] to support immobilizing bacteria for pesticide degradation,[7,8] among other applications, and it has shown promising results. In addition, it presents a porous, spongy texture and many hollows and cavities, which could favor its application as support for enzyme immobilization, fulfilling the requirements of sustainable support.[2,9]

Recent studies report that biodiesel production used ZIF-8, MOF-5, MOF-253, and IRMOF-16 to immobilize different lipases using an adsorption method, with biodiesel yields of 80–85% after 18 hours at a constant temperature.[10–12] On the other hand, in recent years, the coupling between two different materials has gained significant interest due to the physicochemical properties that they can provide, mainly for enzyme immobilization. ZIFs have shown favorable results in terms of compatibility for the coupling of materials.[13,14] Some of these materials, such as Fe_3O_4@ZIF-8, have high-temperature resistance,[15] higher surface area and porosity,[16,17] and better semiconducting properties.[14] However, one of the challenges for coupling and enabling the surface growth of MOFs on a different structure is the functionalization and growth technique.[14] This involves the use of functionalities for the modification of materials, such as in the case of (3-aminopropyl) triethoxysilane (APTES).[18,19] Unfortunately, APTES is toxic and insoluble in water, requiring large amounts of solvents for incorporation. In addition, some materials require pretreatment by adding H_2CO_4 or NaOH to form OH groups, as is the case of pozzolans,[20] which is a significant disadvantage. It is

[a]*Universidad Autónoma del Estado de México, Facultad de Química, Paseo Colón esq. Paseo Tollocan s/n, Toluca, CP 50120, Mexico. E-mail: vvarelag@uaemex.mx; fromeror@uaemex.mx; niztey11@gmail.com*

[b]*Centro de Investigaciones Químicas, UAEM, Av. Univ. 2001, Col. Chamilpa, Cuernavaca, Morelos 62210, Mexico*

[c]*Instituto de Ciencias Físicas, Universidad Nacional Autónoma de México, C.P. 62210 Cuernavaca, Morelos, Mexico. E-mail: naveen@icf.unam.mx*

[d]*Universidad Autónoma del Estado de México, Facultad de Química, Carretera Toluca-Ixtlahuaca Km. 15, Unidad el Cerrillo, Toluca, Estado de México, 50200, Mexico*

[e]*Centro Conjunto de Investigación en Química Sustentable UAEM-UNAM, Carretera Toluca-Atlacomulco Km 14.5, Toluca, Estado de México, 50200, Mexico*

[f]*Centro de Investigación en Ingeniería y Ciencias Aplicadas, UAEM, Av. Univ. 1001, Col. Chamilpa, Cuernavaca, Morelos 62209, Mexico*

† Electronic supplementary information (ESI) available. See DOI: https://doi.org/10.1039/d5ra02711j

crucial to carry out a sustainable synthesis in simple reaction conditions.

For this reason, in this work, it was proposed the implementation of 2-methylimidazole, used for the manufacture of ZIF-8 as a functionalizing agent, which in turn participates as a precursor for the growth of ZIF-8 in tezontle, applying the *in situ* method. Conversely, biodiesel is produced by transesterifying triacylglycerides with methanol or ethanol in the presence of homogeneous primary catalysts, such as NaOH or KOH. However, using this type of catalyst has some drawbacks, such as difficulty purifying the biodiesel and recovering the catalyst. Under this context, using biocatalysts from immobilized lipases facilitates recovery and allows the recyclability of biocatalysts. Currently, enzymatic immobilization processes are expensive, mainly due to the supports used, and some need to be of better quality. An essential strategy to reduce the cost is the multiple reuses of the biocatalyst. This project seeks to synthesize and characterize materials such as ZIF-8 and ZIF-8/tezontle to the immobilization of lipases for their application in the production of biodiesel and, in this way, avoid recovery and recyclability problems of the biocatalyst.

Furthermore, MOFs have been reported to improve enzymatic stability and facilitate immobilization due to their available surface area and composition, avoiding reagents for activating the functional support groups.[21] On the other hand, tezontle is a natural, abundant, environmentally friendly, cheap material that would solve the cost problem. It is worth mentioning that tezontle has yet to be reported as a support for enzyme immobilization, and there are few studies on the use of ZIF-8 as a support for enzyme immobilization and in the production of biodiesel, which leads to the study of new materials. On the other hand, inadequate waste cooking oil management leads to environmental problems, mainly in water. For this reason, biodiesel production from waste cooking oil is proposed.

This work focuses on developing and characterizing efficient and cost-effective materials for enzyme immobilization by improving enzymes' stability and recyclability (Scheme 1). In this work, we have developed highly efficient, stable, resistant, economical, and room temperature reproducible biocatalysts with an enzyme loading efficiency higher up to 91% recyclability efficiency.

2. Materials and methods

2.1. Materials

Zinc nitrate hexahydrate ($Zn(NO_3)_2 \cdot 6H_2O$, Sigma-Aldrich, >98%) as a metal source, 2-methylimidazole (HmIm, $C_4H_6N_2$, Sigma-Aldrich, >99%), sodium formate (NaCOOH, Sigma-Aldrich, >95%) and methanol (MeOH, >95%). For the immobilization process, *Candida rugosa* lipase type VII (Sigma-Aldrich, ≥700 units per mg), dibasic and monobasic potassium phosphates (K_2HPO_4 and KH_2PO_4, Sigma-Aldrich, 99.0%), and ethanol (EtOH, 99.0%) were used. And tezontle, which was acquired in a nursery in Morelos. 4-Nitrophenyl palmitate ($C_{22}H_{35}NO_4$, Sigma-Aldrich, ≥98%) was used as a substrate to evaluate enzymatic activity.

2.2. Synthesis of ZIF-8

The synthesis of ZIF-8 was carried out by the solvothermal method following the technique of Lee *et al.*[17] It consisted of the preparation of a solution of 2-methylimidazole (12 mmol), $Zn(NO_3)_2 \cdot 6H_2O$ (2.6 mmol) and COOHNa (3.6 mmol) in 20 mL of MeOH, which was subjected to a temperature of 120 °C for 4 h in a stainless-steel autoclave. The growth sample was allowed to cool to room temperature for 2 h. Subsequently, it was washed 3 to 5 times with MeOH and allowed to dry at room temperature for recovery and characterization.

2.3. Synthesis of ZIF-8/tezontle

For the coupling of ZIF-8/tezontle, it was necessary to functionalize the crushed tezontle using the functionalization technique reported by Abraha *et al.*[22] with some modifications. A solution of 2-methylimidazole (12 mmol) was prepared in 20 mL of MeOH, adding 2 g of crushed tezontle. Subsequently,

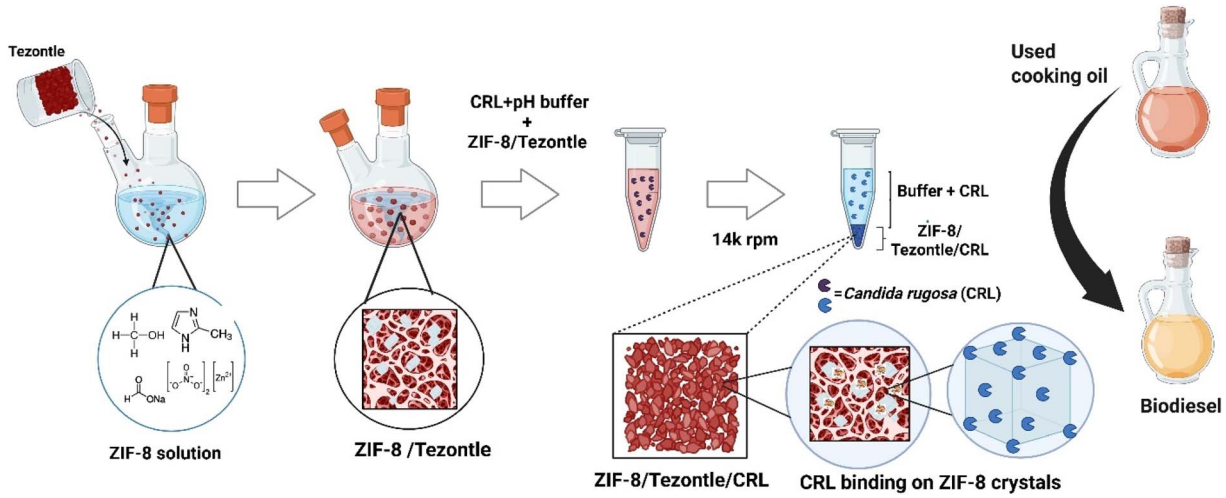

Scheme 1 A schematic representation of the process involved in preparing the biocatalyst ZIF-8/tezontle/CRL and its application in biodiesel conversion from used cooking oils.

the sample was subjected to constant stirring for 8 h at room temperature (25 °C) and recovered at 14 000 rpm. Once the functionalized sample was recovered, a solution of $Zn(NO_3)_2 \cdot 6H_2O$ (2.6 mmol) with COOHNa (3.6 mmol) in 20 mL of MeOH was added, stirring for 8 h at room temperature. The resulting sample was washed 3 times with MeOH and allowed to dry at room temperature for subsequent characterization.

2.4. Enzymatic immobilization by adsorption

Immobilization by adsorption method is one of the simplest since no organic ligands are required for the enzyme/support coupling.[23,24] To carry out this method, a stock lipase solution in phosphate buffer at different pH ranges (4–8). Subsequently, 70 μL of stock solution in 10 mg of support was added, and it was subjected to constant stirring at a temperature of 4 °C for 8 h. The biocatalyst recovered to 14 000 rpm, removing the supernatant for future tests. The immobilized lipase loading (eqn (1)) and enzyme loading efficiency (eqn (2)) were monitored by measuring absorbance in a Thermo Fisher Scientific Evolution 60 UV-visible spectrophotometer at a wavelength of 595 nm by the Bradford method using the BSA (Bovine Serum Albumin) protein assay kit,[25,26] applying eqn (1) and (2).

$$\text{Lipase loading} = C_{ss}\left(\frac{V_{ss} - \text{Abs}_s}{V_{TR} \times \text{Abs}_E}\right) \quad (1)$$

$$\text{Loading efficiency } (\%) = \frac{\text{Lipase loading}}{C_{ss}} \times 100 \quad (2)$$

where C_{ss} is the concentration in the stock solution (mg), V_{ss} is the volume used of the stock solution (μL), Abs_s is the absorbance of the supernatant, V_{TR} is the total volume in for the reaction (μL) and Abs_E is the absorbance of the enzyme.

2.5. Physicochemical characterization of support and biocatalysts

The morphology and elemental composition of the supports and the catalyst were determined by SEM-EDX using a JEOL JCM 6000 scanning electron microscope. For the structural analysis of the supports, the X-ray diffraction (XRD) technique was utilized with an X-ray diffractometer model Rigaku ULTIMA IV considering a step size of 0.02° and a scanning speed of 2° min^{-1}, using CuKα ($\lambda = 0.15418$ nm) as incident radiation. Surface area and pore size analysis were carried out using the BET–BJH method with equipment from Quantachrome Instruments. Each sample (0.1318–0.991 g) was degassed for 16 hours, and the nitrogen adsorption isotherm at 77 K was obtained. The thermogravimetric analysis of the supports was carried out in a NETZSCH thermal analyzer, model STA 449 F3 Jupiter, in a temperature range of 25–800 °C and a ramp of 10 °C min^{-1} in an atmosphere of N_2. The supports and biocatalysts were analyzed in a Varian 660-IR spectrophotometer at room temperature in a 600–4000 cm^{-1} range.

2.6. Enzyme activity and kinetics (V_{max} and K_m)

For this study, the absorbance of free lipase, ZIF-8/lipase, tezontle/lipase and ZIF-8/tezontle/lipase was measured at a wavelength of 410 nm, using a Thermo Fisher Scientific Evolution 60 UV-visible spectrophotometer, considering different temperature ranges, pH, 4-NPP concentration and stability analysis.

2.7. Measurement of enzyme activity by varying temperature and pH

To measure the activity of the biocatalysts, a 50 mM phosphate buffer solution at pH 7 was prepared, taking several aliquots with a determined amount of EtOH, dissolved lipase, and 4 mM 4-NPP. Subsequently, the samples were subjected to a water bath at different temperature ranges (25–60 °C) for 30 minutes (standard time). At the end of this time, a 0.1 M sodium carbonate solution was added and allowed to rest for 1 minute. For recovery, it was centrifuged at 13 000 rpm, preserving the supernatant for later measurement.[25,26] Once the optimum temperature is obtained, only the pH is varied (4–8) using the same methodology.

2.8. Determination of enzyme stability

Having the reaction parameters, the methodology from previous section was carried out, varying only the time (10–120 min) to analyze the stability of the immobilized biocatalysts and the free lipase. It is worth mentioning that a reaction time of 30 min was considered for measuring general activity.

2.9. Kinetic parameters (V_{max} and K_m)

Once the optimal temperature, pH, and time are obtained, the methodology of above section is carried out by varying only the concentration of 4-NPP (0.3–4 mM). To know the kinetic parameters, the Michaelis–Menten model is used. It is worth mentioning that when the logarithmic trend of the data is inadequate, it is necessary to linearize the logarithmic curve of the Michaelis–Menten model through its ordinate at the origin and its slope to determine V_{max} and K_m by implementing the Lineweaver–Burk diagram or analytical calculation.

2.10. Recyclability

For the recyclability study of the biocatalysts recovered (tezontle/lipase, ZIF-8/lipase, and ZIF-8/tezontle/lipase), the enzymatic activity in the hydrolysis of 4-NPP was evaluated for 5 continuous cycles, subjecting them to a temperature of 35 °C for a period of 1 h. The recovery of the immobilized biocatalyst involved washing it with EtOH to remove the solvent, and it was then subjected to centrifugation at 14 000 rpm for 2 minutes. This procedure was carried out twice consecutively. Subsequently, it was left to dry in a desiccator at room temperature for 5 minutes to be stored at 4 °C.[27] To calculate recyclability efficiency (RE), eqn (3) was considered, where E_A is the enzymatic activity (U per mg), and D_R is the desired result (100%).

$$\text{RE } (\%) = \frac{E_A \times 100}{D_R} \quad (3)$$

2.11. Biodiesel production

The enzymatic production of biodiesel involved the use of biocatalysts (tezontle/lipase, ZIF-8/tezontle/lipase, and ZIF-8/lipase) in 10 mg aliquots. These were combined with a mixture of alcohol and oil at varying concentrations (3 : 1, 4 : 1, 6 : 1, and 8 : 1).[28] The process was conducted in a water bath within a sealed reactor to prevent alcohol losses, with stirring at a consistent 200 rpm and a steady temperature of 40 °C for 24 hours.[29,30] The conversion yield (CY) was calculated using eqn (4), where V_{BO} represents the volume of biodiesel obtained, and V_{B100} is the volume of biodiesel assuming 100% transesterification.[31] It is important to note that the conversion was monitored at regular intervals using thin-layer chromatography (TLC).

$$\% \ \mathrm{CY} = \frac{V_{\mathrm{BO}}}{V_{\mathrm{B100}}} \times 100 \tag{4}$$

2.12. Analysis of waste cooking oil (WCO) and biodiesel (BD)

To know the properties of both WCO and BD, it was necessary to perform some quality tests based on the general standard NMX-F-050-SCFI-2013 for vegetable oil[32] and the general standard ASTM D6751 for biodiesel (ESI Table S1†).[29] It is worth mentioning that in this methodology, interest analyses were carried out, such as those mentioned below.

2.12.1. Acidity index (AI). Oils and fats naturally present free acidity, that is, uncombined fatty acids, due to the hydrolysis of some triglycerides. The acid value is the number of milligrams of potassium hydroxide required to neutralize the free fatty acids in 1 g of sample.[33] The result is expressed in milligrams of potassium hydroxide (mg KOH per g) according to the following expression:

$$\mathrm{AI} = \frac{56.1 \times N \times V}{P} \tag{5}$$

where 56.1 is the chemical equivalent of KOH, N is the normality of the KOH solution, V is the spent volume of the KOH solution, and P is the mass of the sample in grams.

To express as a percentage of oleic, palmitic, or lauric fatty acid, the following equation is applied, using the meq. of the reference fatty acid, which is primarily oleic acid:

$$\% \ \mathrm{FFA} = \frac{\mathrm{meq.} \times N \times V}{P} \times 100 \tag{6}$$

where meq. is the chemical milliequivalent of the reference fatty acid (0.282), N is the normality of the KOH solution, V is the volume in mL of spent KOH solution, and P is the weight of the sample in grams. A certain amount of oil and biodiesel was weighed to determine the acid number. Subsequently, a 0.1 N KOH solution was prepared. A mixture of isopropyl alcohol and toluene (v/v) was added, with three drops of phenolphthalein. The sample was titrated with the KOH solution until it was pink.[34] It is worth mentioning that for the WCO, the general Mexican standard NMX-F-101-SCFI-2012 was considered the maximum value, while for the BD, the ASTM D664 standard was considered (ESI Table S1†).[35]

2.12.2. Humidity (H). Humidity mean the mass loss of the oil or fat.[36] The result is expressed in % according to the following expression:

$$\% \ H = \frac{M_1 - M_2}{M_1} \times 100 \tag{7}$$

where M_1 is the mass of the undried sample, and M_2 is the mass of the one without H. A certain amount of oil and biodiesel was weighed in a crucible to determine the H. The samples were subjected to a temperature of 103 °C in a muffle for 3 h. They were then allowed to cool in a desiccator for 30 minutes and weighed again.[37] For the determination of H of the WCO, the maximum value reported in the Mexican standard NMX-F-211-SCFI-2006 was considered, while for the BD, the ASTM D7467 standard was considered (ESI Table S1†).[38]

2.12.3. Analysis of biodiesel Fourier transform infrared spectroscopy (FT-IR). As mentioned in the above section that this characterization technique was used to know the functional groups corresponding to biodiesel. It was carried out in a Varian 660-IR spectrophotometer at room temperature in a wavenumber range of 400–2000 cm^{-1}.

3. Results and discussion

3.1. Scanning electron microscopy with EDX detector (SEM-EDX) of ZIF-8/tezontle and ZIF-8/tezontle/lipase

Using SEM, the morphology of each of the proposed materials was analyzed as shown in Fig. 1a and b it can be seen that tezontle is a porous material with predominant cavities that can measure from 409 nm to 1.88 μm (ref. 6 and 7) and cubic-shaped crystals belonging to ZIF-8 are observed.[38,39] While in Fig. 1c hexagonal-shaped ZIF-8 crystals coupled on the surface of tezontle are observed. Likewise, elements belonging to ZIF-8, such as N and Zn, were identified using EDX (Fig. 1d),[40] which proves that the ZIF-8/tezontle coupling method was favorable.

Likewise, in Fig. 2a, it is observed that within the cavities of the tezontle, the ZIF-8 is incorporated in its cubic form

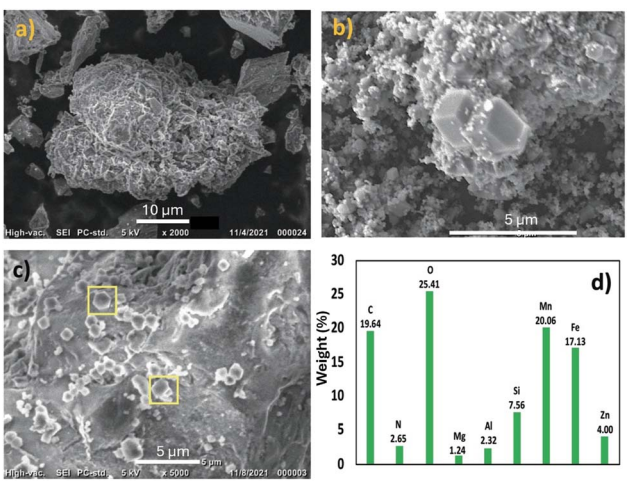

Fig. 1 Micrograph of (a) tezontle, (b) ZIF-8, (c) ZIF-8/tezontle and (d) EDX of ZIF-8/tezontle.

(≈715 nm at 1.42 μm), which may be favorable for the lipase in the recyclability process.[18] It is worth mentioning that this characterization technique was also implemented to check the presence of lipase, observing a slight modification in the structure of ZIF-8/tezontle due to its incorporation into the surface of ZIF-8 (Fig. 2b). This may be due to the functional groups of ZIF-8, which may favor the enzyme/support conjunction.[21,41,42] On the other hand, in Fig. 2c, it is observed that there was an increase of 83% of N compared to Fig. 1d. This is due to the presence of lipase in the ZIF-8/tezontle structure, which also causes the decrease of Zn and Fe by coating the surface and/or its affinity towards these elements.[43,44]

3.2. X-ray diffraction (XRD)

By studying the crystallinity and phases of pristine tezontle and ZIF-8 by XRD, the feasibility of the synthesis method to obtain ZIF-8/tezontle was verified. In Fig. 3, the presence of ZIF-8 was observed in the tezontle structure at angles 7.3°, 12.65° and 17.97° belonging to the planes (100), (211), and (222), like pristine ZIF-8 (JCPDS 00-062-1030).[6,45] In addition, low-intensity patterns are observed in ZIF-8/tezontle compared to tezontle (see the complete diffractogram in Fig. S1 and Table S2†). This is like the case of anorthite (An), which could indicate the formation of ZIF-8 crystals on the surface of tezontle.

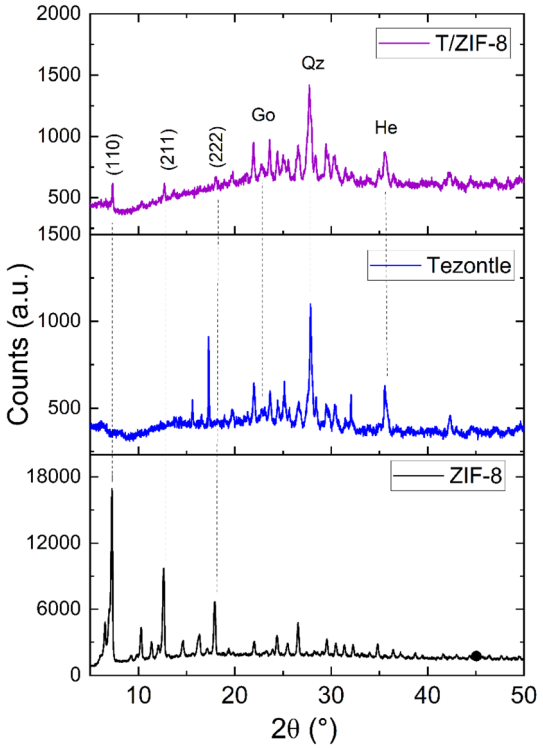

Fig. 3 Comparative diffractogram of ZIF-8/tezontle where the coupling of ZIF-8 in the structure of the tezontle (goethite (Go), quartz (Qz) and hematite (He)).

3.3. Surface area analysis (BET–BJH)

Surface area is crucial in materials for enzyme immobilization due to its influence on physicochemical processes such as adsorption. A larger surface area provides more active sites for the enzyme, allowing the molecules to interact with the substrate and increase the reaction rate. On the other hand, the pore size determines the material's capacity to retain or allow the passage of a substance. If the pore size is too large, the enzyme can detach from the support, which reduces its efficiency.[21] Table 1 presents the surface area and pore size of each support, as determined by the BET–BJH method. It is observed that the surface area of tezontle (6.223 $m^2\ g^{-1}$) is significantly lower compared to ZIF-8

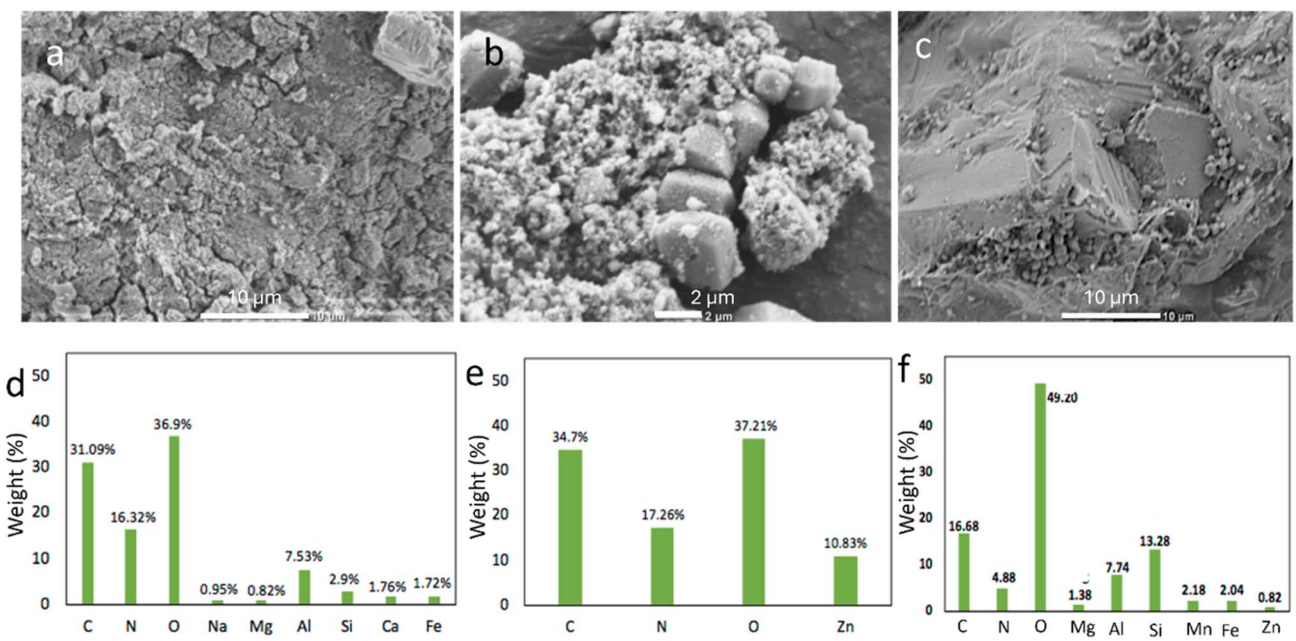

Fig. 2 Micrograph of lipase immobilized (a) tezontle, (b) ZIF-8, (c) ZIF-8/tezontle and their corresponding elemental analysis (d–f) tezontle, ZIF-8 and ZIF-8/tezontle, respectively.

Table 1 Surface properties of biocatalyst support such as tezontle, ZIF-8 and tezontle/ZIF-8

Supports	Surface area ($m^2\ g^{-1}$)	Pore size (nm)	Pore volume ($cm^3\ g^{-1}$)
Tezontle	6.223	152.4	0.0237
ZIF-8	1851	21.5	0.682
ZIF-8/tezontle	119.9	27.2	0.0812

($1851\ m^2\ g^{-1}$). This may be due to the porous and highly organized structure of ZIF-8. In addition, it is observed that ZIF-8/tezontle has a larger surface area ($119.9\ m^2\ g^{-1}$) than tezontle, which indicates that the empty spaces were filled by covering irregularities, creating a new interface between the two materials; it means an additional surface area is added to the already existing one, increasing the total surface area.

On the other hand, the pore size of ZIF-8/tezontle (27.2 nm) is smaller than tezontle (152.4 nm) with a particle size ranging between 409 nm and 1.8 μm and similar to ZIF-8 (21.5 nm), which may indicate the obstruction or filling that occurred on the surface of tezontle, thus proving that the larger the pore size, the smaller the surface area and *vice versa*. It is worth mentioning that ZIF-8 and ZIF-8/tezontle are mesoporous materials, which favors the enzyme since it has an approximate size of 3 to 7 nm (depending on the type of enzyme), which facilitates the interaction of the enzyme and the substrate and the enzyme/substrate binding due to the surface area available.[1,2] Additionally, this would facilitate the diffusion of the final product, in this case, BD. At the same time, the tezontle, being a macroporous material, can directly affect the enzyme, as mentioned above, facilitating the detachment of the enzyme during the reaction (for more information, see the adsorption isotherms in Fig. S2†). Another fundamental data that we can appreciate in Table 1 is the pore volume; this factor determines the amount of enzyme that can be retained in the support (see Enzyme loading section). It is observed that ZIF-8 has a pore volume of $0.682\ cm^3\ g^{-1}$, being superior to tezontle ($0.0237\ cm^3\ g^{-1}$) and ZIF-8/tezontle ($0.0812\ cm^3\ g^{-1}$). This may be due to the fact that ZIF-8 has a sodalite type structure (SOD) and has the presence of internal porous cavities,[2,5] while ZIF-8/tezontle had a slight increase in comparison to tezontle; this may be due to the distribution of the pores, since there may be smaller pores that contribute to the total volume or that the material has a complex shape that generates interconnected spaces.[5]

3.4. Thermogravimetric analysis (TGA)

The TGA evaluated the thermal stability of ZIF-8/tezontle, and the thermogram of the prepared supports is shown in Fig. 4 (for more details, see Fig. S3–S5†). As can be observed, the weight of the ZIF-8/tezontle remained constant during the reaction, indicating a total weight loss of 1.8% within the range of 400–800 °C, corresponding to the ZIF-8 and tezontle compounds. Likewise, tezontle remains almost unchanged, losing a total of 2% of its weight when the temperature increases from 100 to 200 °C due to its purity. Subsequently, it decreases by 1.4% in weight in a range of 200–520 °C due to the presence of

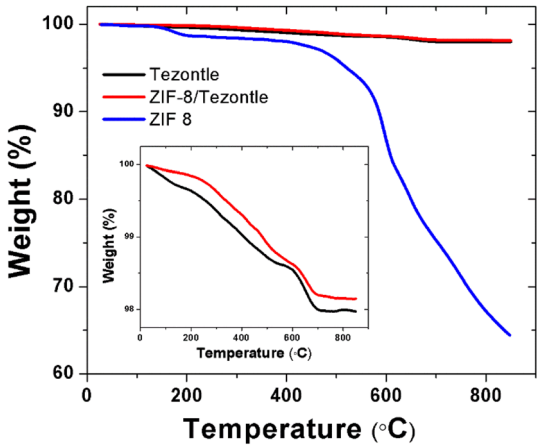

Fig. 4 Thermogravimetric analysis of the supports ZIF-8/tezontle, tezontle, ZIF-8, and comparative inset thermogram.

compounds containing aluminum (elite, cordierite, and albite, among others).[30] Furthermore, from 540 to 800 °C, it suffers a decrease in weight of 0.6%, corresponding to iron compounds (goethite, illite, cordierite, and hematite).[30,32] On the other hand, the thermogram of pristine ZIF-8 shows a total weight loss of 35.5%, with a 1.3% weight loss over the temperature range of 200–400 °C, indicating that ZIF-8 remains stable up to 400 °C, as reported in the literature.[32] After decomposition, the remaining weight (≈30%) corresponds to the formation of zinc oxide (ZnO), which happens due to the complete oxidation or degradation of ZIF-8 (2-methylimidazole decomposes and zinc ions combined with oxygen in the air to form ZnO). Additionally, it can be observed that ZIF-8/tezontle has a significantly lower weight than pristine ZIF-8. This may be because there is a lower amount of ZIF-8 in the tezontle.

3.5. Fourier transform infrared spectroscopy (FT-IR) of ZIF-8/tezontle and ZIF-8/tezontle/lipase

The functional groups corresponding to each of the supports (ZIF-8, tezontle, and ZIF-8/tezontle) were analyzed by FTIR (view

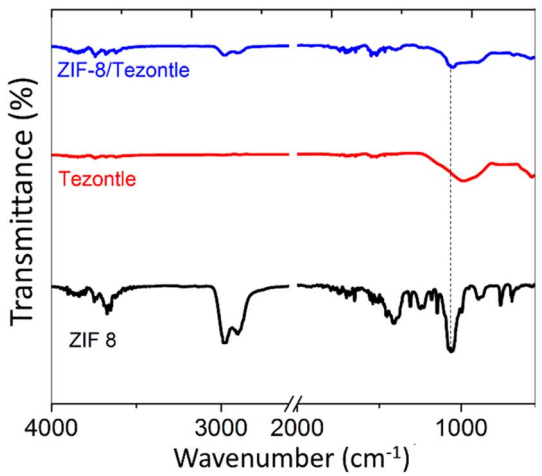

Fig. 5 FTIR spectra of the pristine supports with their respective functional groups (Tables 1 and 2).

Table 2 ZIF-8 functional groups

Wavenumber (cm^{-1})	Functional groups
692	Zn–N
754	Zn–O
756	HmIm rings
1397	C–H (HmIm)
1423	C=N
1457	C–N
1576	Axial deformation of C=N

Table 3 Tezontle functional groups

Wavenumber (cm^{-1})	Functional groups
≈500	FeO
≈600	CaO
750	Si–C
950	Si–OH/Si–O
1033	Si–O–Si
1100	Si–O

Fig. 5). Table 2 shows the functional groups corresponding to ZIF-8, proving that its coupling in the tezontle structure was favorable when bands belonging to HmIm (756–1576 cm^{-1})[17,39,40] were observed. On the other hand, Table 3 shows the functional groups present in tezontle, such as FeO and SiO, which favor immobilization, as the enzymes have an affinity towards metals. On the other hand, the functional groups associated with the enzyme are observed between the bands at 1640–1660 cm^{-1} and 3370–3380 cm^{-1}, corresponding to C=O and N–H stretching (see Fig. 6).[16,29] In the case of tezontle, the band of the functional group corresponding to the enzyme cannot be observed; this may be due to the presence of cavities and the enzyme/support complex. This suggests that lipase detachment may have occurred. However, the presence of an enzyme can also be verified by SEM-EDX techniques (see Fig. 2).

3.6. Enzyme loading

To calculate the loading and efficiency of immobilized lipase, eqn (1) and (2) were used, considering the initial concentration based on the stock solution (70 μL) and the appropriate pH conditions. Subsequently, the absorbance was measured at 595 nm. The enzyme loading efficiency of ZIF-8 was ≈80%, higher than tezontle (74%) and ZIF-8/tezontle (71%); this may be due to the surface area, pore volume (view Section 3.3) and functional groups.[30] However, studies have reported that ZIF-8 can achieve efficiency higher than 90%, depending on the structure obtained during its synthesis.[6,45] Likewise, tezontle demonstrated a loading efficiency of 74%, which is superior to that of ZIF-8/tezontle. This may be due to the porosity; however, it could also generate the detachment of the enzyme during the reaction, in addition to showing agglomeration, as it lacks available active sites due to its low surface area.[30] On the other hand, ZIF-8/tezontle shows an enzyme loading efficiency of 71%. This result is favorable, as the absence of lipase agglomeration improves its activity compared to pristine tezontle (see Fig. 2a). However, this result may indicate that a small amount of ZIF-8 is present in the tezontle since the enzyme tends to be coupled with ZIF-8, as shown in Fig. 2b.

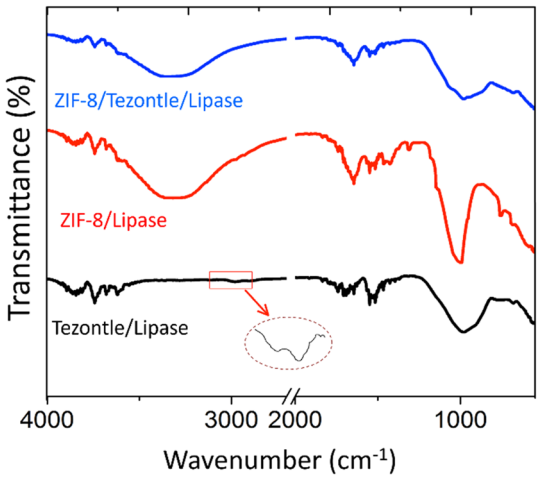

Fig. 6 FTIR spectrum of the lipase incorporated ZIF-8, tezontle, and ZIF-8/tezontle.

3.7. Enzymatic activity

This section evaluated the biocatalysts by varying the temperature, pH, time, and concentration of 4-NPP. It is worth mentioning that the biocatalyst of interest is ZIF-8/tezontle/lipase. However, each biocatalyst (ZIF-8/lipase and tezontle/lipase) will be briefly described.

3.7.1. Determination of activity by varying temperature. One of the most important parameters in biocatalysis is temperature, as it directly influences the enzyme's shape and enzymatic activity, allowing for diffusion between the enzyme and substrate. At low temperatures, activity decreases because the molecules move more slowly, resulting in fewer collisions between the enzyme and the substrate. In contrast, at high temperatures, activity increases up to an optimum point, reaching the maximum reaction rate. However, if this temperature is exceeded, the enzyme tends to denature.[21] The incubation temperature is presented in Fig. 7 showing a higher relative activity at a temperature ranging between 35 °C and 40 °C for the three types of biocatalysts (97% for ZIF-8/tezontle/lipase, 98% for tezontle/lipase and 98% ZIF-8/lipase respectively) (Fig. 7a) and free lipase (93%) (Fig. 7b), being the ideal operating temperature for *Candida rugosa* lipase and living organisms.[30]

On the other hand, the decrease in enzymatic activity of the immobilized biocatalysts compared to free lipase can be observed. This may be due to the coupling of the enzyme during the immobilization method and its subsequent handling.[22,46] Additionally, as the temperature increases, enzymatic activity decreases, indicating the denaturation of the enzyme.

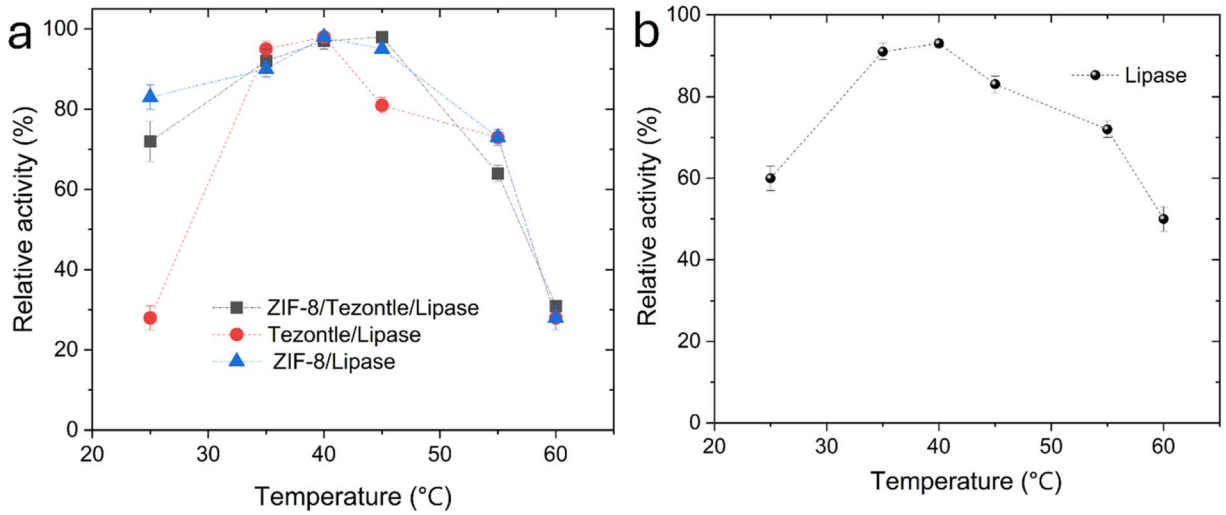

Fig. 7 Comparison of the relative activity of (a) the immobilized biocatalysts and (b) the free lipase varying the temperature.

3.7.2. Determination of activity by varying pH. pH plays a critical role in the shape and structure of the enzyme[18] and is directly influenced by the substrate.[47,48] In Fig. 8a, it is observed that the optimal reaction pH is 7 for the immobilized biocatalysts, showing relative activity of 92% for ZIF-8/tezontle/lipase and 98% for ZIF-8/lipase. In contrast, for tezontle/lipase, the activity is 67%. This may be due to agglomeration, which favors denaturation.[18,49] On the other hand, the free lipase showed a relative activity of 91% (Fig. 8b), which is higher than that of ZIF-8/tezontle/lipase; this may be due to the immobilization method. Furthermore, the decrease in activity observed at pH 8, with ZIF-8/tezontle/lipase showing 47% activity and ZIF-8/lipase showing 40%, can be attributed to the interaction between the enzyme and the support. The relative activity of 98% for tezontle/lipase further supports this observation. The changes in the enzyme's structure and its interaction with the substrate may indicate denaturation by agglomeration, which favors the formation of aggregates that hinder the substrate's access to the enzyme's active site. These results give us a clear understanding that the lipase is bound to ZIF-8 due to its surface area and chemistry. This finding explains the observed similarity in efficiency between ZIF-8/lipase and ZIF-8/tezontle as shown in Fig. 2b.

3.7.3. Stability analysis with respect to time. To verify the stability, it was necessary to know the optimal reaction conditions measuring the activity at different incubation time intervals (10–20 min). In Fig. 9a, it is observed that tezontle/lipase presents better activity in overtime, showing 98% (at 10 min) being 4% higher than ZIF-8/tezontle/lipase (94%). Likewise, as mentioned, ZIF-8/lipase (94%) may be due to the contact between the lipase and the substrate. However, it showed similar ZIF-8/tezontle/lipase activities throughout the reaction. Furthermore, there was a significant decrease in the first period (10 to 20 min), showing relative activity of 93% for ZIF-8/

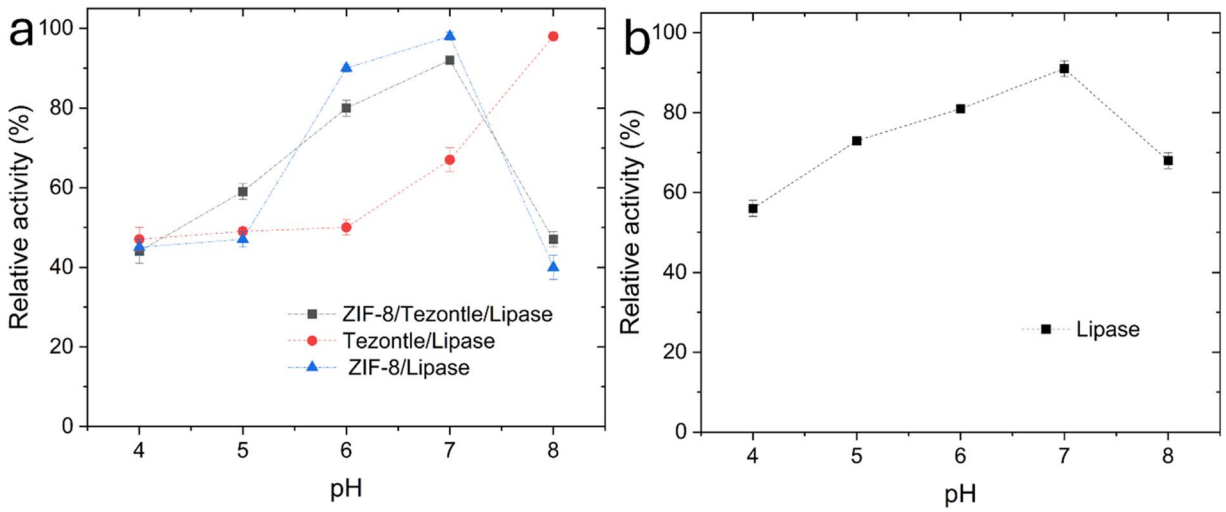

Fig. 8 Comparison of the relative activity of (a) the immobilized biocatalysts and (b) free lipase varying the pH.

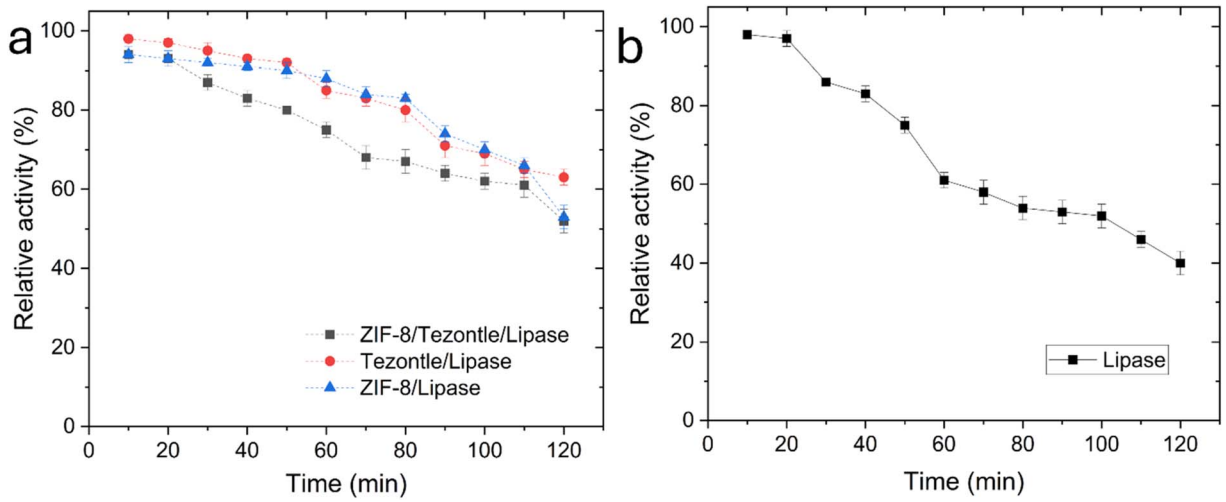

Fig. 9 Comparison of the relative activity of (a) the immobilized biocatalysts and (b) free lipase varying the incubation time.

tezontle/lipase, 93% for ZIF-8/lipase and 97% for tezontle/lipase. As time passes, the drop-in activity is more progressive until 120 minutes, where the activity is 52% for ZIF-8/tezontle/lipase, 53% for ZIF-8/lipase and 63% for tezontle/lipase coupling with the biocatalyst of interest. It is worth mentioning that the decrease in activity is also due to the low availability of substrate (4-NPP) and to the change in pH due to the increase in products.[50,51]

3.7.4. Kinetic parameters (V_{max} and K_m). The comparison of the enzymatic activity of the biocatalysts *versus* the substrate concentration (4-NPP) is presented in Fig. 10. At 0.5 mM, more significant relative activity was obtained for ZIF-8/tezontle/lipase (92%) and ZIF-8/lipase (98%) (Fig. 10a). At the same time, for tezontle/lipase it shows a relative activity of 67% at this concentration (Fig. 10a). However, by increasing the concentration to 1 mM its activity increases (98%), this may be since there is a significant amount of lipase on the support that interacts with the substrate[50,52] or it may even indicate that the enzyme concentration is limited or when the enzyme is saturated. The same happens with free lipase, which, being pure, requires a significant amount of substrate; in this case, an activity of 98% was obtained at a concentration of 3 mM (Fig. 10b). It is worth mentioning that lipase has a high activity because it is free. There is no obstruction to its interaction with the substrate.

Table 4 shows the maximum velocity (V_{max}) of the biocatalysts, being 0.233 μmol min^{-1} or ZIF-8/tezontle/lipase and 0.246 μmol min^{-1} for ZIF-8/lipase, while for tezontle/lipase it is 0.190 μmol min^{-1}. While the Michaelis constant (K_m) was of 0.114 mM for ZIF-8/tezontle/lipase, 0.051 mM for ZIF-8/lipase, and 0.031 mM for tezontle/lipase. On the other hand, the free lipase shows a V_{max} of 0.666 μmol min^{-1} and a K_m of 0.147 mM higher than ZIF-8/tezontle/lipase. It is worth mentioning that a high K_m value represents low affinity and a weak association between enzyme and substrate, and even that the acquired lipase is not 100% pure.

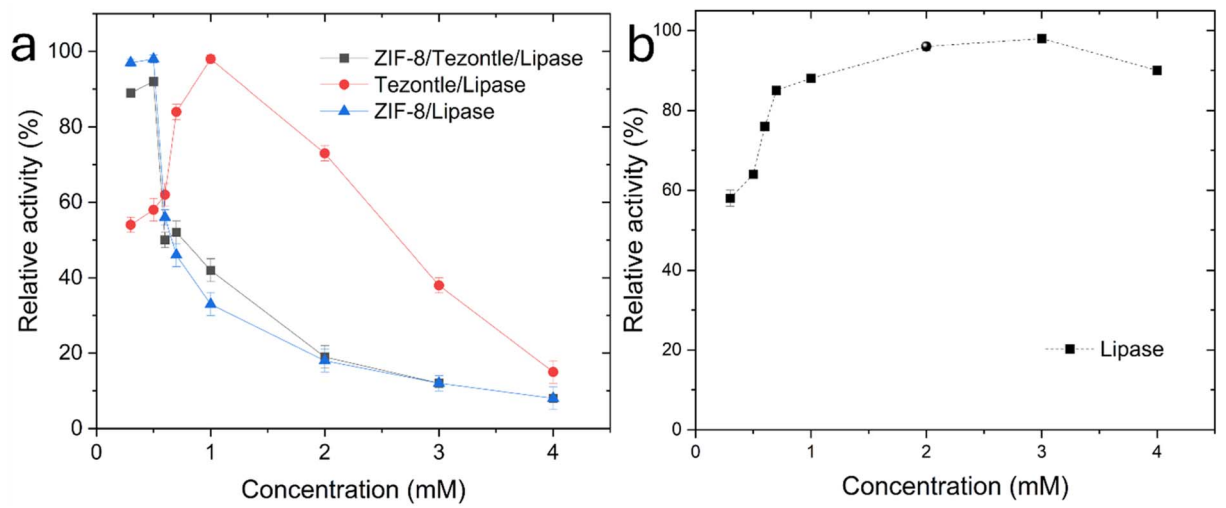

Fig. 10 Enzymatic activity varying the concentration of (a) ZIF-8/tezontle/lipase, tezontle/lipase, ZIF-8/lipase and (b) free lipase, respectively.

Table 4 Reaction conditions of the biocatalysts for the quantification of enzymatic activity

	Reaction conditions					
Catalysts	Temperature (°C)	pH	Reaction time (min)	Concentration 4-NPP (mM)	V_{max} (μmol min^{-1})	K_m (mM)
ZIF-8/tezontle/lipase	35–40	7	30	0.5	0.233	0.114
Tezontle/lipase	35–40	8	30	1	0.190	0.031
ZIF-8/lipase	35–40	7	30	0.5	0.246	0.051
Free lipase	35–40	7	30	3	0.666	0.147

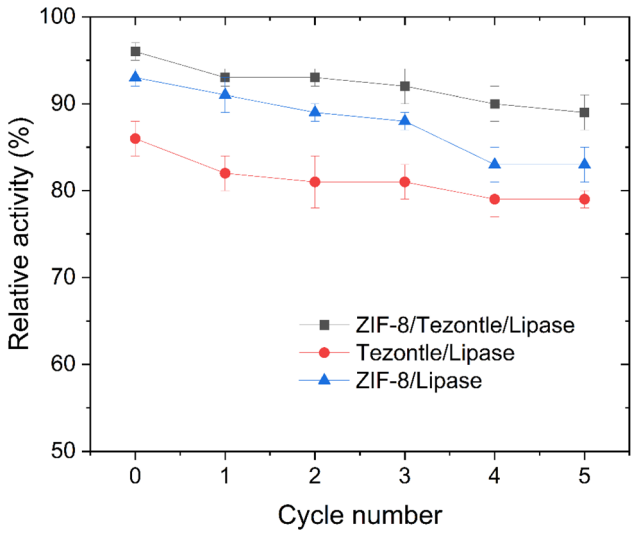

Fig. 11 Recyclability of the immobilized biocatalysts, comparing the enzymatic activity and the activity efficiency.

3.8. Recyclability

One factor that interferes with the recyclability process is the affinity between the enzyme and the support (enzyme/support). The support protects the enzyme against reaction conditions such as temperature, pH, solvents used in the recovery method, and even the storage of the biocatalyst.[21,53] In Fig. 11, it is observed that ZIF-8/tezontle/lipase after 5 continuous cycles (89%) (as presented in other studies reported in Table 5), did not show a significant loss of activity compared to the initial cycle (96%). This means that ZIF-8/tezontle is a stable material capable of protecting lipase. Likewise, ZIF-8/lipase (83%) and tezontle/lipase (79%) showed low efficiency when used 5 times compared to ZIF-8/tezontle/lipase.

3.9. Biodiesel production

To produce BD, an alcohol : oil mixture was prepared at different ratios (3 : 1, 4 : 1, 6 : 1, and 8 : 1), obtaining better conversion yields at a ratio of 4 : 1 (Fig. 12). For ZIF-8/tezontle/lipase, a yield of 91.26% was obtained (view Table 5), while for ZIF-8/lipase, it showed a result of 92.25%. This may be due to the enzyme/substrate complex, as no cavities obstruct the enzyme, allowing for better diffusion. The same phenomenon occurred with the free lipase, yielding 97.26%. On the other hand, the tezontle/lipase showed a yield of 89.23%, indicating that it has a significant contact between enzyme/substrate; however, the agglomeration of the enzyme and the lack of functional groups do not favor the enzyme/substrate union, which facilitates its detachment, causing a lower yield and low activity.[21]

Table 5 Comparison of results with published literature with their respective characteristics and reaction conditions

			Reaction conditions					
Biocatalyst	Immobilization method	Substrate	Temp. (°C)	Alcohol : oil molar ratio	Reaction time (h)	Initial conversion yield (%)	Recyclability (cycles)	Ref.
ANL (*Aspergillus niger* lipase) @M-ZIF-8	Encapsulation	Soybean oil	40	4 : 1	24	>90	5	54
ANL (*Aspergillus niger* lipase) @M-ZIF-8-PDMS	Encapsulation	Soybean oil	45	4 : 1	2–4	>90	5	55
CZ-600-M-0.5@TLL	Adsorption	Soybean oil	40	4 : 1	12	>90	5	56
Lipase@ZIF-8	Encapsulation	Undisrupted microalgae	—	—	3	>50	5	57
BCL (*Burkholderia cepacia* lipase)-ZIF-8	Adsorption	Soybean oil	40	4 : 1	12	93.4	8	58
Fe_3O_4@MIL-100(Fe) + *Candida rugosa* lipase	Covalent bonding	Soybean oil	40	4 : 1	60	92.3	5	59
Lipase (QLM from *Alcaligenes* sp.) @Bio-MOF	—	Sunflower oil	50	8 : 1	4	>80	5	60
ZIF-8/tezontle/lipase	Adsorption	WCO	40	4 : 1	24	91.26	5	Present study

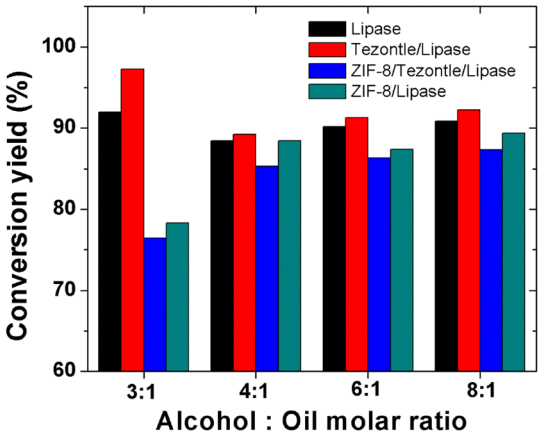

Fig. 12 Conversion yield of BD varying the alcohol : oil molar ratio.

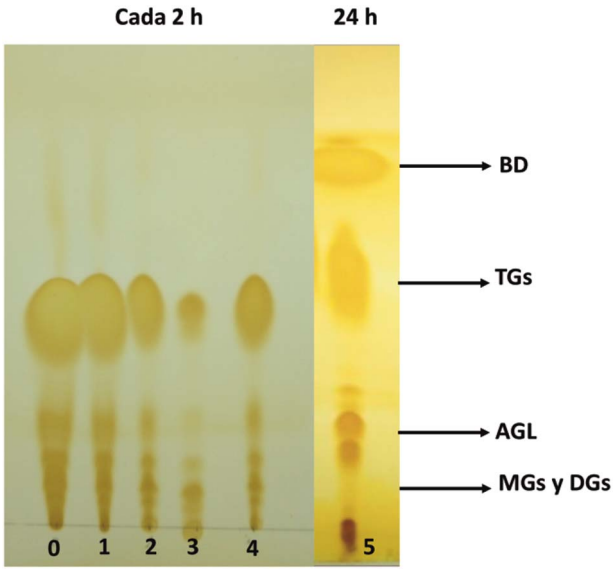

Fig. 13 TLC of the oil/BD conversion process using ZIF-8/tezontle/lipase for 24 h at mild reaction conditions.

It is worth noting that the conversion was monitored by thin-layer chromatography (TLC), with aliquots taken every 2 hours, resulting in a total phase separation time of 2 minutes. In Fig. 13, point 0 represents the WCO, which serves as a reference for analyzing the transesterification process. Points 1, 2, 3, and 4 represent the enzymatic transesterification process using immobilized *Candida rugosa*, with the presence of BD observed in point 5. The total reaction time was 24 h, resulting in a retention factor of 0.94.

3.10. Quality parameters

The acidity index, humidity, density, and viscosity are essential parameters in the BD area. Therefore, for the reason, it was considered to analyze these quality parameters according to the general standard NMX-F-050-SCFI-2013 (for WCO) and ASTM D6751 (for BD), showing the results obtained in Table 6.

To calculate the AI, eqn (5) was considered, resulting in 0.67 mg KOH per g and 0.2% FFA for the WCO. This indicates that it is a quality oil, complying with the NMX-F-101-2006 standard. Likewise, it is observed that the AI of BD was reduced to 0.22 mg KOH per g and the percentage of FFA to 0.1%, a result below the ASTM D664 standard (maximum allowed: 0.5 mg KOH per mg) (view ESI Table S1†). This may indicate that the oil/BD conversion was favorable.[34,61] Conversely, H is a parameter related to AI. The lower the H, the lower the AI.[34,62] For this reason, the H analysis was conducted, yielding a result of 0.05% for the WCO, which complied with the NMX-F-211-SCFI-2006 standard. In comparison, while the BD presented an H of 0.075%, which is a value of ≈26% above the ASTM D2709 standard (maximum allowed: 0.05%). This may be due to the fact that biodiesel is hygroscopic, *i.e.*, it can absorb water from the environment;[34] however, this value did not affect the AI. Other parameters listed in Table 5 are density and viscosity. It is observed that WCO has a density of 897 kg m^{-3}, while BD has a density of 750 kg m^{-3}. This may be due to the origin of the oil, including the temperature.[54] The kinematic viscosity is related to the temperature and composition of fatty acids such as long chains, degrees of unsaturation, and functional groups of BD,[62] being lower (4.027 mm^2 s^{-1}) compared to WCO (32.40 mm^2 s^{-1}); this value is below the ASTM D445 standard (view ESI Table S1†). It is worth mentioning that this analysis was carried out using the BD obtained with ZIF-8/tezontle/lipase, the biocatalyst of interest.

3.11. Analysis of biodiesel by Fourier transform infrared spectroscopy (FT-IR)

The characteristics of the FT-IR spectral analysis of the WCO and the synthesized BD are shown in Fig. 14, observing chemically similar spectra. The carbonyl functionality (–C=O) was observed in the 1800 cm^{-1} and 1700 cm^{-1} regions for both samples. The C=O stretching of WCO was observed at the wave number of 1750 cm^{-1} due to the presence of FFA.[63] In the transesterification process of WCO, the C=O stretching band of ethyl ester shifted to 1742 cm^{-1}.[64] The fingerprint region (1500–900 cm^{-1}) showed different functional groups between WCO and BD. The characteristic band at ~1353 cm^{-1} belongs to both samples' bending vibration of the $-CH_2$ and $-CH_3$ groups. However, at 1435 cm^{-1}, the asymmetric bending $-CH_3$ was observed in the case of BD, being absent in the WCO.[62] The band at 1197 cm^{-1} is due to the stretching vibration of $-OCH_3$ of the BD (ethyl ester), absent in the WCO.[65] The characteristic –C–O stretching bands are found at 1169 and 1235 cm^{-1} for both samples. However, the intensity was reduced due to the elimination of triglycerides and FFA forming ethyl ester in the BD.[66] The C–C double bond functional group was found at 1650 cm^{-1} for both samples. However, the band intensity for BD was reduced. This is due to the reduction of the double bond character during the chemical reaction.[63] The saturated C–C bond stretching (–C–H) was observed at position 723 cm^{-1} with lower intensity for BD than for WCO. This decrease confirmed the reduction in chain length during the transesterification process.

Table 6 Quality parameters of waste cooking oil (WCO) and biodiesel (BD)

Name	AI (mg KOH per g)	FFA (%)	H (vol%)	Density (g mL^{-1})	Kinematic viscosity (mm^2 s^{-1})
WCO	0.67	0.2	0.05	0.897	32.40
BD	0.22	0.1	0.075	0.750	4.027

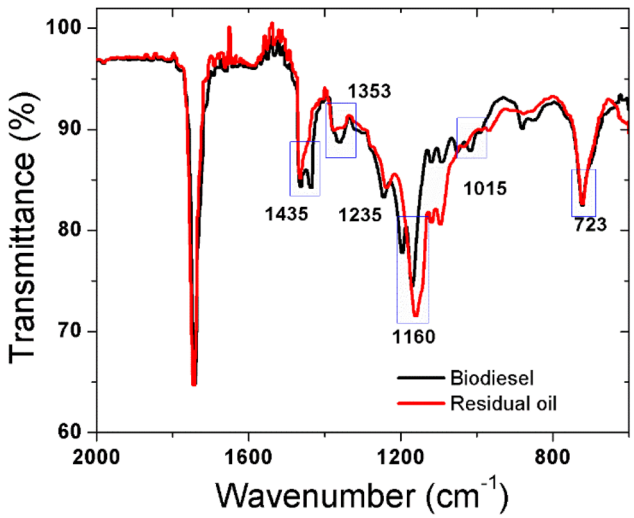

Fig. 14 Comparison of FT-IR transmission spectra of WCO and biodiesel.

4. Conclusions

According to the results reported by XRD and MEB-EDX, it was confirmed that the synthesis method applied for coupling ZIF-8 in tezontle was favorable, with tiny cubic crystals of ≈approximately 715 nm at 1.42 μm being observed. BET analysis of ZIF-8/tezontle (119.9 m^2 g^{-1}) revealed a favorable pore size (27.2 nm), as determined by the BJH method, which is suitable for enzyme immobilization. On the other hand, the presence of the immobilized enzyme in the holes of the tezontle is confirmed, where the highest concentration of ZIF-8 is found, allowing for the recyclability of the biocatalyst and maintaining an activity of more than 80% for 5 consecutive cycles. Likewise, the FTIR analysis confirms that the immobilization process was favorable, as evidenced by the presence of functional groups characteristic of the enzyme (C=O and N–H). In the thermogravimetric analysis, it is observed that ZIF-8/tezontle exhibits greater thermal stability compared to ZIF-8 (total mass loss of 35.5%) and tezontle (0.2% mass loss), which favors enzymatic activity (relative activity = 98%). According to the kinetic analysis, it is deduced that ZIF-8/tezontle/lipase exhibits a favorable affinity to the substrate (K_m = 0.114 mM), indicating that it does not significantly block the interaction, allowing for a strong interaction between the lipase and the substrate. Using *Candida rugosa* to produce BD requires mild reaction conditions, achieving an efficiency greater than 90% in production, as described in the literature. This is an advantage, as it leads to energy savings and improved economics on an industrial scale.

As for the results of the WCO and the BD, it is observed that they comply with the quality parameters of the ASTM technique, obtaining an acidity index of 0.67 mg KOH per g for the oil and 0.2 mg KOH per g for the BD (limit: 0.5 mg KOH per g); 0.05% humidity for the oil and 0.075% (limit: 0.05%) for the BD respectively. Based on the above, it is verified that the enzyme defines the reaction conditions, not the support, but this interferes with its recyclability and stability. ZIF-8/tezontle showed favorable structural, morphological, thermal, and chemical results for enzyme immobilization (load greater than 60%), allowing enzyme/support binding, which would prevent lipase leaching.

Data availability

The data that support the findings of this study are available from the corresponding author upon reasonable request.

Author contributions

Yetzin Rodríguez-Mejía: conceptualization, methodology, investigation, writing – original draft, visualization. Naveen Kumar Reddy Bogireddy: investigation, writing – review & editing, visualization. Fernando Romero-Romero: supervision, conceptualization, methodology, investigation, reviewing – original draft. M. V. Basavanag-Unnamatla: investigation, writing – review & editing. Vivechana Agarwal: supervision and methodology. Victor Varela-Guerrero: supervision, funding acquisition, writing – review & editing.

Conflicts of interest

The authors declare that they have no financial interests or personal relationships that could have appeared to influence the work reported in this paper.

Acknowledgements

The authors acknowledge the financial support given by DGAPA-UNAM (Dirección General de Asuntos del Personal Académico) under Project No. PAPIIT-IA202324. The authors would like to acknowledge the technical support provided by Jose Juan Ramos-Hernandez and Maura Casales Diaz of ICF, UNAM, for BET analysis. Y. R.-M. acknowledge Secretaría de Ciencia, Humanidades, Tecnología e Innovación (SECIHTI) for postdoctoral fellowship.

References

1 E. M. Otazo Sánches, A. Ortiz Polo and R. M. Richards Uribe, Ponce Lira, Br, Avances en impacto, tecnología y toxicología ambiental, in *Mater. Funcionales Para La Remoción Iones Metálicos Contam. Del Agua*, Universidad Autónoma del Estado de Hidalgo, Hidalgo, México, 1st edn, 2011, pp. 1–158.

2 P. Vargas Tapia, J. Z. Castellanos Ramos, J. d. J. Muñoz Ramos, P. Sánchez García, L. Tijerina Chávez, R. M. López Romero, C. Martínez Sánchez and J. L. Ojodeagua Arredondo, Effect of particle size on some physical properties of tezontle (volcanic rock) from the state of Guanajuato, *Agric. Tec. Mex.*, 2008, **34**, 323–331.

3 C. San Martín-Hernández, V. M. Ordaz-Chaparro, P. Sánchez-García, M. T. Beryl Colinas-Leon and L. Borges-Gómez, Calidad de tomate (Solanum lycopersicum L.) producido en hidroponia con diferentes granulometrías de tezontle, *Agrociencia*, 2012, **46**, 243–254.

4 S. Demirdag, I. Ugur and S. Sarac, The effects of cement/fly ash ratios on the volcanic slag aggregate lightweight concrete masonry units, *Constr. Build. Mater.*, 2008, **22**, 1730–1735, DOI: **10.1016/j.conbuildmat.2007.05.011**.

5 J. Acevedo-Dávila, L. M. Torres-Treviño and L. Y. Gómez Z., Tezontle aggregate substitute optimization in building blocks mixture, *Electron. Robot. Automot. Mech. Conf. CERMA 2007 – Proc.*, 2007, pp. 307–311, DOI: **10.1109/CERMA.2007.4367704**.

6 A. Tejeda, A. Barrera and F. Zurita, Adsorption capacity of a volcanic rock—Used in constructed wetlands—For carbamazepine removal, and its modification with biofilm growth, *Water*, 2017, **9**, 721, DOI: **10.3390/w9090721**.

7 G. Yáñez-Ocampo, E. Sánchez-Salinas and M. L. Ortiz-Hernández, Removal of methyl parathion and tetrachlorvinphos by a bacterial consortium immobilized on tezontle-packed up-flow reactor, *Biodegradation*, 2011, **22**, 1203–1213, DOI: **10.1007/s10532-011-9475-z**.

8 G. Yañez-Ocampo, E. Sanchez-Salinas, G. A. Jimenez-Tobon, M. Penninckx and M. L. Ortiz-Hernández, Removal of two organophosphate pesticides by a bacterial consortium immobilized in alginate or tezontle, *J. Hazard. Mater.*, 2009, **168**, 1554–1561, DOI: **10.1016/j.jhazmat.2009.03.047**.

9 B. P. Lira, A. O. Polo, E. M. O. Sánchez, E. R. Ruiz, O. A. A. Sandoval, F. P. García and C. A. G. Ramírez, Physical characterization of an extensive volcanic rock in México: "red tezontle" from Cerro de la Cruz, in Tlahuelilpan, Hidalgo, *Acta Univ.*, 2013, **23**, 9–16, **http://www.redalyc.org/articulo.oa?id=41628340002**.

10 J. Sahar, M. Farooq, A. Ramli, A. Naeem, N. S. Khattak and Z. A. Ghazi, Highly efficient heteropoly acid decorated SnO_2@Co-ZIF nanocatalyst for sustainable biodiesel production from Nannorrhops ritchiana seeds oil, *Renewable Energy*, 2022, **198**, 306–318, DOI: **10.1016/j.renene.2022.08.005**.

11 S. K. Bhatia, R. Gurav, T. R. Choi, H. J. Kim, S. Y. Yang, H. S. Song and Y. H. Yang, Conversion of waste cooking oil into biodiesel using heterogeneous catalyst derived from cork biochar, *Bioresour. Technol.*, 2020, **302**, 122872, DOI: **10.1016/j.biortech.2020.122872**.

12 M. Narasimhan, M. Chandrasekaran, S. Govindasamy and A. Aravamudhan, Heterogeneous nanocatalysts for sustainable biodiesel production: A review, *J. Environ. Chem. Eng.*, 2021, **9**, 104876, DOI: **10.1016/j.jece.2020.104876**.

13 H. Konnerth, B. M. Matsagar, S. S. Chen, M. H. G. Prechtl, F. K. Shieh and K. C. W. Wu, Metal-organic framework (MOF)-derived catalysts for fine chemical production, *Coord. Chem. Rev.*, 2020, **416**, 213319, DOI: **10.1016/j.ccr.2020.213319**.

14 W. Zhan, Q. Kuang, J. Zhou, X. Kong, Z. Xie and L. Zheng, Semiconductor@Metal–Organic Framework Core–Shell Heterostructures: A Case of ZnO@ZIF-8 Nanorods with Selective Photoelectrochemical Response, *J. Am. Chem. Soc.*, 2013, **135**, 1926–1933, DOI: **10.1021/ja311085e**.

15 A. Schejn, T. Mazet, V. Falk, L. Balan, L. Aranda, G. Medjahdi and R. Schneider, Fe_3O_4@ZIF-8: Magnetically recoverable catalysts by loading Fe_3O_4 nanoparticles inside a zinc imidazolate framework, *Dalton Trans.*, 2015, **44**, 10136–10140, DOI: **10.1039/c5dt01191d**.

16 Y. Hu, H. Zhou, L. Dai, D. Liu, S. Al-Zuhair and W. Du, Lipase Immobilization on Macroporous ZIF-8 for Enhanced Enzymatic Biodiesel Production, *ACS Omega*, 2021, 6–11, DOI: **10.1021/acsomega.0c05225**.

17 Y. R. Lee, M. S. Jang, H. Y. Cho, H. J. Kwon, S. Kim and W. S. Ahn, ZIF-8: A comparison of synthesis methods, *Chem. Eng. J.*, 2015, **271**, 276–280, DOI: **10.1016/j.cej.2015.02.094**.

18 C. R. Lin, O. S. Ivanova, D. A. Petrov, A. E. Sokolov, Y. Z. Chen, M. A. Gerasimova, S. M. Zharkov, Y. T. Tseng, N. P. Shestakov and I. S. Edelman, Amino-functionalized Fe_3O_4@SiO_2 core-shell magnetic nanoparticles for dye adsorption, *Nanomaterials*, 2021, **11**, 2371, DOI: **10.3390/nano11092371**.

19 M. Jafarzadeh, E. Soleimani, P. Norouzi, R. Adnan and H. Sepahvand, Preparation of trifluoroacetic acid-immobilized Fe_3O_4@SiO_2-APTES nanocatalyst for synthesis of quinolines, *J. Fluorine Chem.*, 2015, **178**, 219–224, DOI: **10.1016/j.jfluchem.2015.08.007**.

20 A. G. N. Wamba, E. C. Lima, S. K. Ndi, P. S. Thue, J. G. Kayem, F. S. Rodembusch, G. S. dos Reis and W. S. de Alencar, Synthesis of grafted natural pozzolan with 3-aminopropyltriethoxysilane: preparation, characterization, and application for removal of Brilliant Green 1 and Reactive Black 5 from aqueous solutions, *Environ. Sci. Pollut. Res.*, 2017, **24**, 21807–21820, DOI: **10.1007/s11356-017-9825-4**.

21 Y. Rodríguez Mejía, F. Romero Romero, M. V. Basavanag Unnamatla, M. F. Ballesteros Rivas and V. Varela Guerrero, Metal-Organic Frameworks as bio- and heterogeneous catalyst supports for biodiesel production, *Rev. Inorg. Chem.*, 2023, **43**(2), 323–355, DOI: **10.1515/revic-2022-0014**.

22 Y. W. Abraha, C. W. Tsai and E. H. G. Langner, De novo syntheses of multi-linker Zn- and Co-based ZIFs with

application in CO_2 fixation, *Microporous Mesoporous Mater.*, 2022, **346**, 112319, DOI: 10.1016/j.micromeso.2022.112319.
23 S. Datta, L. R. Christena and Y. R. S. Rajaram, Enzyme immobilization: an overview on techniques and support materials, *3 Biotech*, 2013, **3**, 1–9, DOI: 10.1007/s13205-012-0071-7.
24 M. Arroyo, Inmovilizacion de enzimas. Fundamentos, metodos y aplicaciones, *Ars Pharm.*, 1998, **39**, 111–127.
25 Y. Hu, L. Dai, D. Liu and W. Du, Rationally designing hydrophobic UiO-66 support for the enhanced enzymatic performance of immobilized lipase, *Green Chem.*, 2018, **20**, 4500–4506, DOI: 10.1039/c8gc01284a.
26 S. Velasco-Lozano, F. López-Gallego, R. Vázquez-Duhalt, J. C. Mateos-Díaz, J. M. Guisán and E. Favela-Torres, Carrier-free immobilization of lipase from Candida rugosa with polyethyleneimines by carboxyl-activated cross-linking, *Biomacromolecules*, 2014, **15**, 1896–1903, DOI: 10.1021/bm500333v.
27 S. García Gonzáles Estudio y Preparación de Biocatalizadores Basados En Lipasa Inmovilizada En Diferentes Soportes, *Aplicación a la Obtención de Biodiesel*, 2017.
28 J. R. Baccaro Díaz, Evaluación de Rendimiento de Biodiesel Elaborado a Partir de Aceite de Palma Africana (Elaeis Guineensis) y Etanol Anhidro de Caña de Azúcar (Saccharum Officinarum), *Zamorano*, 2007, pp. 1–34.
29 M. Adnan, K. Li, L. Xu and Y. Yan, X-shaped ZIF-8 for immobilization rhizomucor miehei lipase via encapsulation and its application toward biodiesel production, *Catalysts*, 2018, **8**, 1–14, DOI: 10.3390/catal8030096.
30 S. M. Roberts and A. J. Gibb, *Introduction to Enzymes, Receptors and the Action of Small Molecule Drugs*, 2013, DOI: 10.1016/B978-0-12-397176-0.00001-7.
31 P. R. Santagapita, Estabilidad de enzimas en medios de movilidad molecular. Impacto de interacciones con azúcares y biopolímeros y de la encapsulación, Facultad de Ciencias Exactas y Naturales, PhD thesis, Universidad de Buenos Aires, 2010, http://digital.bl.fcen.uba.ar.
32 Y. Hu, L. Dai, D. Liu, D. Liu, W. Du and W. Du, Hydrophobic pore space constituted in macroporous ZIF-8 for lipase immobilization greatly improving lipase catalytic performance in biodiesel preparation, *Biotechnol. Biofuels*, 2020, **13**, 1–10, DOI: 10.1186/s13068-020-01724-w.
33 Y. Wu and H. Zhang, NMX-F-101-SCFI-2012 – Alimentos – Aceites y grasas vegetales o animales – Determinación de ácidos grasos libres, México, 2012.
34 E. Arenas, S. M. Villafán-Cáceres, Y. Rodríguez-Mejía, J. A. García-Loyola, O. Masera and G. Sandoval, Biodiesel Dry Purification Using Unconventional Bioadsorbents, *Processes*, 2021, **9**, 194, DOI: 10.3390/pr9020194.
35 ASTM International, ASTM D664-18e2: Standard test method for acid number of petroleum products by potentiometric titration, 2018.
36 B. No and A. Preenvasados, NMX-F-083-1986, Alimentos, determinación de humedad en productos alimenticios, México, 1998.
37 ASTM International, ASTM D2709: Water and sediment in middle distillate fuels by centrifuge, 2018.
38 O. M. Linder-Patton, T. J. De Prinse, S. Furukawa, S. G. Bell, K. Sumida, C. J. Doonan and C. J. Sumby, Influence of nanoscale structuralisation on the catalytic performance of ZIF-8: A cautionary surface catalysis study, *CrystEngComm*, 2018, **20**, 4926–4934, DOI: 10.1039/c8ce00746b.
39 H. Zhang, M. Zhao, Y. Yang and Y. S. Lin, Hydrolysis and condensation of ZIF-8 in water, *Microporous Mesoporous Mater.*, 2019, **288**, 109568, DOI: 10.1016/j.micromeso.2019.109568.
40 F. Hillman, J. M. Zimmerman, S. M. Paek, M. R. A. Hamid, W. T. Lim and H. K. Jeong, Rapid microwave-assisted synthesis of hybrid zeolitic-imidazolate frameworks with mixed metals and mixed linkers, *J. Mater. Chem. A*, 2017, **5**, 6090–6099, DOI: 10.1039/c6ta11170j.
41 M. Bilal, Y. Zhao, T. Rasheed and H. M. N. Iqbal, Magnetic nanoparticles as versatile carriers for enzymes immobilization: A review, *Int. J. Biol. Macromol.*, 2018, **120**, 2530–2544, DOI: 10.1016/j.ijbiomac.2018.09.025.
42 M. Bilal and H. M. N. Iqbal, Chemical, physical, and biological coordination: An interplay between materials and enzymes as potential platforms for immobilization, *Coord. Chem. Rev.*, 2019, **388**, 1–23, DOI: 10.1016/j.ccr.2019.02.024.
43 M. W. Thompson, Regulation of zinc-dependent enzymes by metal carrier proteins, *BioMetals*, 2022, **35**, 187–213, DOI: 10.1007/s10534-022-00373-w.
44 D. J. Reilley, M. R. Hennefarth and A. N. Alexandrova, The Case for Enzymatic Competitive Metal Affinity Methods, *ACS Catal.*, 2020, **10**, 2298–2307, DOI: 10.1021/acscatal.9b04831.
45 A. Schejn, L. Balan, V. Falk, L. Aranda, G. Medjahdi and R. Schneider, Controlling ZIF-8 nano- and microcrystal formation and reactivity through zinc salt variations, *CrystEngComm*, 2014, **16**, 4493–4500, DOI: 10.1039/c3ce42485e.
46 N. M. Nurazzi, N. Abdullah, M. N. F. Norrrahim, S. H. Kamarudin, S. Ahmad, S. S. Shazleen, M. Rayung, M. R. M. Asyraf, R. A. Ilyas and M. Kuzmin, Thermogravimetric Analysis (TGA) and Differential Scanning Calorimetry (DSC) of PLA/Cellulose Composites, *Polylactic Acid-Based Nanocellulose Cellul. Compos.*, 2022, pp. 145–164, DOI: 10.1201/9781003160458-7.
47 Y. R. Mejía and N. K. Reddy Bogireddy, Reduction of 4-nitrophenol using green-fabricated metal nanoparticles, *RSC Adv.*, 2022, **12**, 18661–18675, DOI: 10.1039/d2ra02663e.
48 N. K. Reddy Bogireddy, Y. R. Mejia, T. M. Aminabhavi, V. Barba, R. H. Becerra, A. D. Ariza Flores and V. Agarwal, The identification of byproducts from the catalytic reduction reaction of 4-nitrophenol to 4-aminophenol: A systematic spectroscopic study, *J. Environ. Manage.*, 2022, **316**, 115292, DOI: 10.1016/j.jenvman.2022.115292.
49 A. Ulu, Metal–organic frameworks (MOFs): a novel support platform for ASNase immobilization, *J. Mater. Sci.*, 2020, **55**, 6130–6144, DOI: 10.1007/s10853-020-04452-6.

50 J. L. DeForest, The influence of time, storage temperature, and substrate age on potential soil enzyme activity in acidic forest soils using MUB-linked substrates and l-DOPA, *Soil Biol. Biochem.*, 2009, **41**, 1180–1186, DOI: 10.1016/j.soilbio.2009.02.029.

51 R. K. Scopes, Enzyme Activity and Assays, *ELS*, 2002, 1–6, DOI: 10.1038/npg.els.0000712.

52 S. García Gonzáles, Estudio y Preparación de Biocatalizadores Basados en Lipasa Inmovilizada en Diferentes Soportes, *Aplicación a la Obtención de Biodiesel*, 2017, http://oa.upm.es/47807/1/TFG_SERGIO_GARCIA_GONZALEZ.pdf.

53 L. Casas-Godoy, S. Duquesne, F. Bordes, G. Sandoval and A. Marty, Lipases: an overview, in *Lipases Phospholipases: Methods and Protocols*, ed. G. Sandoval, Springer, 2012, pp. 3–30, DOI: 10.1007/978-1-61779-600-5_1.

54 Y. Hu, H. Zhou, L. Dai, D. Liu, S. Al-Zuhair and W. Du, Lipase Immobilization on Macroporous ZIF-8 for Enhanced Enzymatic Biodiesel Production, *ACS Omega*, 2021, 6–11, DOI: 10.1021/acsomega.0c05225.

55 Y. Hu, L. Dai, D. Liu, D. Liu, W. Du and W. Du, Hydrophobic pore space constituted in macroporous ZIF-8 for lipase immobilization greatly improving lipase catalytic performance in biodiesel preparation, *Biotechnol. Biofuels*, 2020, **13**, 1–9, DOI: 10.1186/s13068-020-01724-w.

56 Y. Shi, H. Zhou, L. Dai, D. Liu, W. Du, E. Sowan, H. Taher, M. S. Mozumder and S. Al-Zuhair, Preparation of Ordered Macroporous ZIF-8-Derived Magnetic Carbon Materials and Its Application for Lipase Immobilization, *Enzyme Microb. Technol.*, 2024, **14**, 110243, DOI: 10.1016/j.enzmictec.2023.110243.

57 E. Sowan, H. Taher, M. S. Mozumder and S. Al-Zuhair, ZIF-8 as support for enhanced stability of immobilized lipase used with a thermoresponsive switchable solvent to simplify the microalgae-to-biodiesel process, *Enzyme Microb. Technol.*, 2023, **167**, 110243, DOI: 10.1016/j.enzmictec.2023.110243.

58 M. Adnan, K. Li, J. Wang, L. Xu and Y. Yan, Hierarchical ZIF-8 toward immobilizing burkholderia cepacia lipase for application in biodiesel preparation, *Int. J. Mol. Sci.*, 2018, **19**, 1424, DOI: 10.3390/ijms19051424.

59 W. Xie and M. Huang, Enzymatic production of biodiesel using immobilized lipase on core-shell structured Fe_3O_4@MIL-100(Fe) composites, *Catalysts*, 2019, **9**, 850, DOI: 10.3390/catal9100850.

60 Q. Q. Li, Y. Chen, S. Bai, X. Shao, L. Jiang and Q. Q. Li, Immobilized lipase in bio-based metal-organic frameworks constructed by biomimetic mineralization: A sustainable biocatalyst for biodiesel synthesis, *Colloids Surf., B*, 2020, **188**, 110812, DOI: 10.1016/j.colsurfb.2020.110812.

61 G. Anastopoulos, Y. Zannikou, S. Stournas and S. Kalligeros, Transesterification of vegetable oils with ethanol and characterization of the key fuel properties of ethyl esters, *Energies*, 2009, **2**, 362–376, DOI: 10.3390/en20200362.

62 S. A. García-Muentes, C. Francisco Lafargue-Pérez, C. Benigno Labrada-Vázquez, C. Manuel Díaz-Velázquez and C. A. E. S. del Campo-Lafita, Propiedades fisicoquímicas del aceite y biodiesel producidos de la Jatropha curcas L. en la provincia de Manabí, Ecuador, *Rev. Cubana Quim.*, 2017, **30**, 143–159.

63 S. Samanta and R. R. Sahoo, Waste Cooking (Palm) Oil as an Economical Source of Biodiesel Production for Alternative Green Fuel and Efficient Lubricant, *Bioenergy Res.*, 2021, **14**, 163–174, DOI: 10.1007/s12155-020-10162-3.

64 I. P. Soares, T. F. Rezende, R. C. Silva, E. V. R. Castro and I. C. P. Fortes, Multivariate calibration by variable selection for blends of raw soybean oil/biodiesel from different sources using Fourier transform infrared spectroscopy (FTIR) spectra data, *Energy Fuels*, 2008, **22**, 2079–2083, DOI: 10.1021/ef700531n.

65 N. G. Siatis, A. C. Kimbaris, C. S. Pappas, P. A. Tarantilis and M. G. Polissiou, Improvement of biodiesel production based on the application of ultrasound: Monitoring of the procedure by FTIR spectroscopy, *JAOCS, J. Am. Oil Chem. Soc.*, 2006, **83**, 53–57, DOI: 10.1007/s11746-006-1175-1.

66 M. A. Dubé, S. Zheng, D. D. McLean and M. Kates, A comparison of attenuated total reflectance-FTIR spectroscopy and GPC for monitoring biodiesel production, *JAOCS, J. Am. Oil Chem. Soc.*, 2004, **81**, 599–603, DOI: 10.1007/s11746-006-0948-x.